An Experimental Study of the Structural Effect on the Nanosecond Nonlinear Optical Response of O-Doped Polycyclic Aromatic Hydrocarbons (PAHs)

Ioannis Papadakis[1,2], *Zoi Bouza*[1,2], *Aristeidis Stathis*[1,2], *Ioannis Orfanos*[1,2], *Stelios Couris*[1,2 *], *Tanja Miletić*[3] and *Davide Bonifazi*[3]

[1]*Physics Department, University of Patras, 26504 Patras, Greece*

[2]*Institute of Chemical Engineering Sciences (ICE-HT), Foundation for Research and Technology-Hellas (FORTH), P.O. Box 1414, Patras 26504, Greece*

[3]*School of Chemistry, Cardiff University, Park Place, CF10 3AT Cardiff, UK*

**email: couris@iceht.forth.gr*

Abstract

The nonlinear optical response of some O-doped PAHs is systematically investigated in the present work aiming to understand the influence of structural effects on their nonlinear optical response. In that view, the third-order nonlinear optical properties of these PAHs were measured under 4 ns, visible (532 nm) and infrared (1064 nm) laser excitation. The O-doped PAHs were found exhibiting large saturable absorption and negative sign nonlinear refraction under visible excitation, both increasing with the addition of naphtalene units and with the number of O-atoms. Their nonlinear optical response was found to be negligible under infrared excitation. Similar measurements performed on thin films of these PAHs have shown that they maintain their large nonlinear optical response even in solid state, confirming their high potential for opto-electronic and photonic applications.

Introduction

Polycyclic aromatic hydrocarbons (PAHs) with tailored linear and nonlinear optical (NLO) properties are excellent candidates for organic optoelectronics.[1–3] The carbon networks of PAHs are also viewed as graphene precursors and model compounds to study and decipher different fundamental structure-property relationships which are occurring in graphene(s) and graphene-like structures.[4,5] In fact, small PAHs, with sizes of 1-5 nm, are named as graphene molecules, while larger size PAHs, with sizes *e.g.* up to100 nm, are called nano-graphenes or nano-ribbons and PAHs with even larger sizes are usually regarded as graphene (sheet), the limits between the different terminologies being rather indiscernible and loosely defined. Furthermore, PAHs can be also viewed as polymers, which can be highly conductive, their conductivity being tunable with their size and the arrangement of the fused hydrocarbon rings, thus covering the whole range from conducting to insulating polymers. In addition, to this semiconducting behavior of PAHs the effective tunability of their molecular HOMO-LUMO gap makes them attractive for applications in optoelectronics as their optical properties can be tuned accordingly to meet the specific needs of some particular application (*e.g.* field effect transistors, solar cells, *etc.*).[6,7]

To exploit the optoelectronic properties of PAHs, several synthetic strategies have been proposed aiming, among other things, to tune efficiently PAHs' bandgap. These strategies are based on the exploitation of different structural parameters of PAHs, as for example the change of the size, the planarity, the edges of the carbon framework, the type of the peripheral functionalization (*e.g.* by inserting electron-donating or -accepting substituents), the change of the aromatic properties of the constituting monomeric units (*e.g.* by selective doping of the carbon framework with heteroatoms), *etc*. In view of potential optoelectronic applications, this latter approach is of significant interest since the replacement of selected carbon atoms by isostructural/isoelectronic analogues leaves the carbon framework rather untouched, as it

creates minor structural modifications, while it can drastically affect the optoelectronic properties of the molecule.[8] In that view, recently, the synthesis of a series of oxygen-containing π-extended PAHs was reported, in which two polyaromatic hydrocarbon substructures were bridged through furanyl[9–11] or pyranopyranyl[11,12] linkages featuring tunable opto-electronic properties.

In particular, in a previous work we reported on the synthesis and characterization of O-doped PAHs based on perylene units with optical absorption and emission properties effectively tailored through the fine tuning of both, the π-extension of the carbon scaffold and the oxygen linkages, covering the visible absorption and emission spectral region.[11] A direct consequence of the above described is the modification of the nonlinear optical (NLO) response of these PAHs arising from, both, the changes of their UV-Vis-NIR absorption spectra and the respective geometrical issues occurring (*i.e.*, size, extent of charge delocalization, aromaticity, planarization of the carbon framework, *etc*.). In fact, the NLO properties of O-doped PAHs investigated in solutions by the Z-scan technique, by employing visible (532 nm), 35 ps laser pulses showed significant second hyperpolarizabilitiy values depending on the molecular planarity and the HOMO–LUMO energy gap. In this context, a detailed study of the NLO response of these O-doped PAHs was initiated aiming to shed light on the fundamental structure-property relationships under different excitation regimes. In the present work, the transient NLO response of furanyl and pyranopyranyl PAHs (Figure 1) is studied under excitation with visible nanosecond laser pulses. In addition, their NLO properties (*i.e.*, NLO absorption and refraction) were investigated and determined employing 4 ns, visible (532 nm) and infrared (1064 nm) laser pulses.

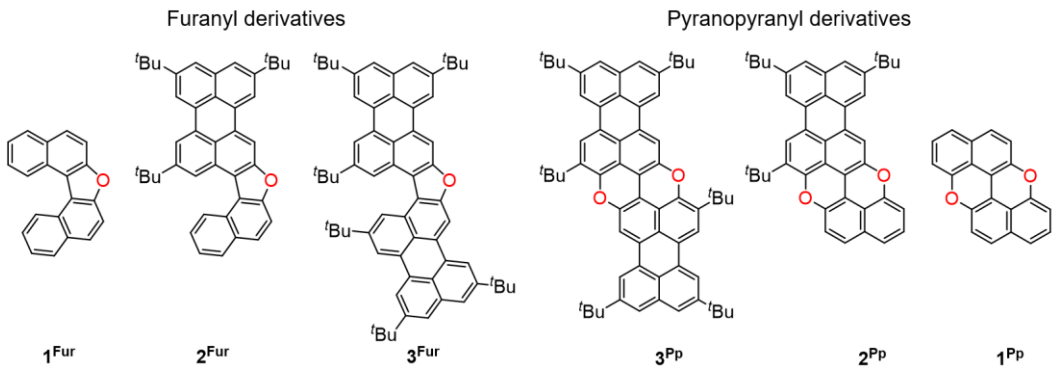

Figure 1. Chemical structure of investigated O-doped PAHs: *Furanyl* derivatives ***1-3***^{Fur} (left) and *pyranopyranyl* derivatives ***1-3***^{Pp} (right).

Experimental Materials

The synthesis and characterization of molecules ***1***$^{Fur/Pp}$***-3***$^{Fur/Pp}$ which are investigated in this work have been recently reported elsewhere.[11] For the study of their nonlinear optical (NLO) response and the determination of their nonlinear optical properties under nanosecond laser excitation, different concentrations of toluene solutions were prepared and placed in 1 mm quartz cells. Using part of these solutions, thin films of the O-doped PAHs were prepared on glass substrates by spin-coating using different experimental conditions (*e.g.* 1000 and 700 rpm, for 30 and 40 s, respectively). The glass substrates were previously carefully cleaned with acetone, ethanol and water, by means of ultrasonic bath and dried under nitrogen atmosphere. Compounds ***1-3***$^{Fur/Pp}$ were solubilized in an appropriate volume of PMMA solution in toluene (*c*=60 mg/mL) and sonicated for 10 min prior to use. The PMMA solution was prepared dissolving 600 mg of PMMA (Polymethylmethacrylate), approx. M.W. 15000 (ACROS Organics, CAS: 9011-14-7, Cat. No. 190690500) in 10 mL of toluene (Spectroscopic grade, *Alfa Aesar*) through sonication (20 min). The films' thicknesses were measured by a Dektak XT™ stylus profilometer. The films prepared using 1000 rpm for 30 s had an average thickness of 350-550 nm, while those prepared using 700 rpm for 40 s were ca. 600-800 nm thick. In

general, all films exhibited good homogeneity and reasonable surface smoothness, as confirmed by naked eye inspection and by detailed profilometry measurements. Both, solutions and films of O-doped PAHs, unirradiated and irradiated ones, were found to be very stable in time. The corresponding UV-Vis-NIR absorption spectra in solution and thin film, measured by a JASCO V-670 spectrophotometer are presented in Figure 2.[11] As shown, all samples exhibited a series of strong absorption peaks, located in the spectral region between 800 to 250 nm, corresponding to the strong π-π* excitations, with the lowest energy absorption band assigned to the HOMO-LUMO electronic transition.

Concerning the absorption spectra of *furanyl* PAHs shown in Figure 2a, the absorption spectrum of the less conjugated ***1***^{Fur} exhibits well-defined narrow profile electronic transitions (located at 326, 340 and 356 nm) while the addition of a naphtalene unit resulted to ***2***^{Fur} produced a less well-resolved absorption bands system with the stronger absorption band located at 477 nm having a bathochromic shift of 121 nm (ε=47300 $M^{-1}cm^{-1}$) with respect to the less conjugated ***1***^{Fur}. Further addition to the ***2***^{Fur} core of one additional naphthalene unit leads to ***3***^{Fur}, exhibiting an additional shift of 57 nm, thus shifting the strongest absorption band peak at 534 nm (ε=97400 $M^{-1}cm^{-1}$). Besides, as shown in Table 1, PAHs ***1***^{Fur}, ***2***^{Fur} and ***3***^{Fur} have very high fluorescence quantum yields Φ_{fl}, *ca*. 0.88, 0.84 and 0.80 respectively, suggesting their high efficiency in reemitting a very large portion of the light they absorb.

Table 1. Optical properties of *furanyl* and pyrano*pyranyl* PAHs studied in toluene solutions (data taken from reference 11).

PAH	λ_{max} [nm][a]	σ [×10^{-17} cm^2]	ε [M^{-1} cm^{-1}]	Φ (%)	τ (ns)
1^{Fur}	356	13	34 000	0.47	-
2^{Fur}	477	18.1	47 300	0.84	3.0
3^{Fur}	534	37.3	97 400	0.80	3.0
1^{Pp}	444	6.6	17 300	0.62	5.0
2^{Pp}	556	13.9	36 300	0.50	3.8
3^{Pp}	639	25.4	66 400	0.52	2.2

[a] Wavelength of the lowest-energy electronic transition in toluene.

As far as it concerns the absorption spectra of the *pyranyl* compounds (see Figure 2b), the simplest one, ***1^{Pp}***, exhibits also well-defined narrow profile electronic transitions, the strongest one being located at about 444 nm (ε=17300 $M^{-1}cm^{-1}$), while the next derivative, ***2^{Pp}***, due to its more extended π-system, exhibits a strong bathochromic shift of about 112 nm relative to ***1^{Pp}***, with the stronger band shifted to 556 nm (ε=36300 $M^{-1}cm^{-1}$). Interestingly, the absorption spectrum of the next *pyranyl* PAH, *i.e.* ***3^{Pp}***, displays a more drastic bathochromic shift of 195 nm compared with ***1^{Pp}***, its strongest absorption band being shifted at 639 nm. It is worth to mention that the *pyranyl* PAHs are in general characterized by relatively lower quantum yields, compared to their *furanyl* counterparts as can be seen in Table 1, the fluorescence quantum yields of ***1^{Pp}***, ***2^{Pp}*** and ***3^{Pp}*** having been reported to be 0.62, 0.50 and 0.52 respectively. Lastly, it is worth to notice, that ***3^{Pp}*** exhibits a shift of 105 nm in respect to the corresponding *furanyl* compound ***3^{Fur}***, due to its higher degree of planarization.

Another interesting observation resulting from the inspection of the absorption spectra of studied PAHs of Figure 2, concerns the broadening of the characteristic absorption bands of the pyranopyranyl (***1-3^{Pp}***) derivatives thin films compared to the furanyl (***1-3^{Fur}***) derivatives. In fact, Pp derivatives, either in solution or in thin films exhibited more broadening compared to the furanyl molecules indicating the more extended aggregation which occurs in the case of pyranopyranyl molecules in agreement with other reports.[11]

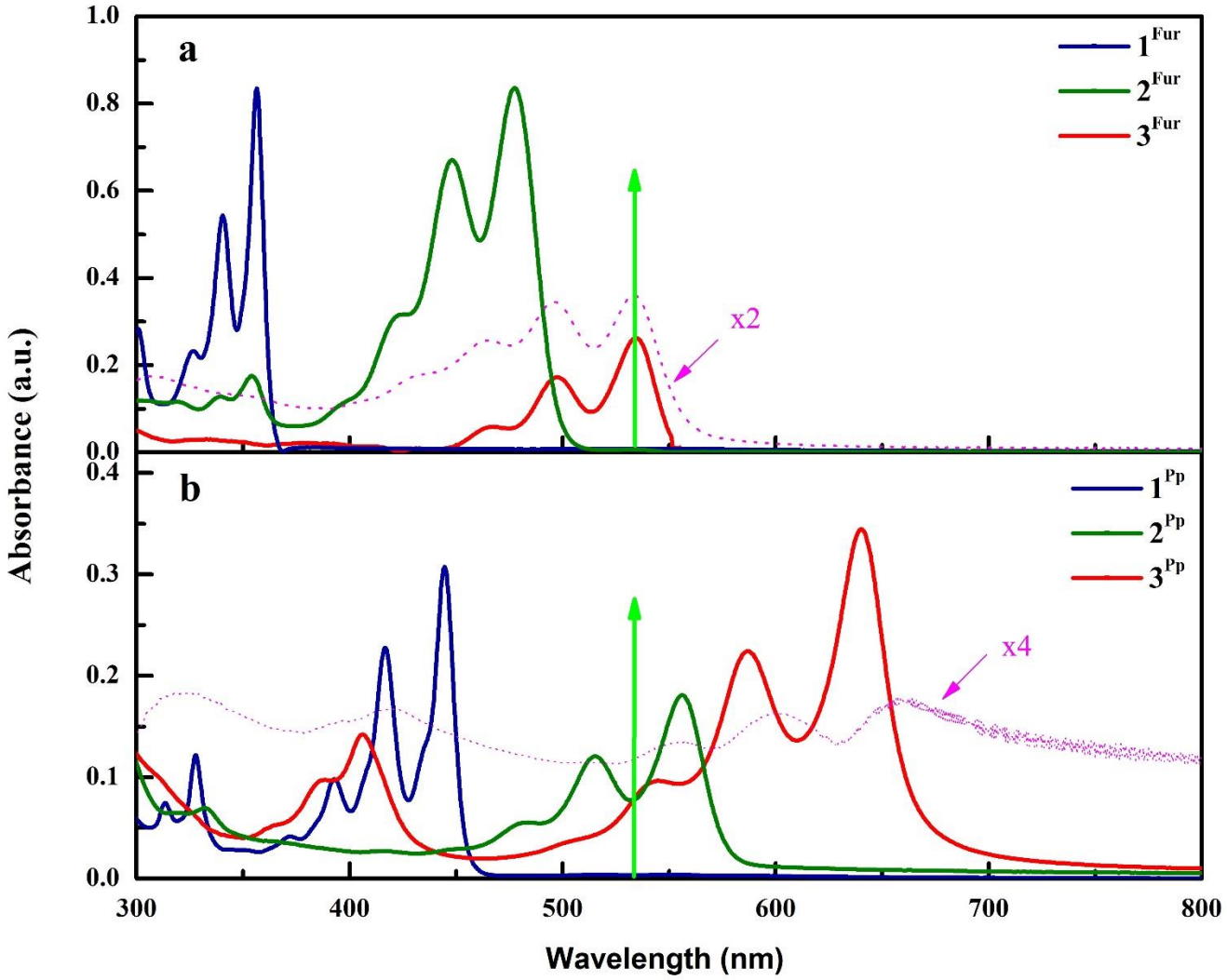

Figure 2. UV-Vis-NIR absorption spectra of toluene solutions of: a) $\boldsymbol{1^{Fur}}$, $\boldsymbol{2^{Fur}}$, $\boldsymbol{3^{Fur}}$, b) $\boldsymbol{1^{Pp}}$, $\boldsymbol{2^{Pp}}$, $\boldsymbol{3^{Pp}}$. The spectra with the dotted lines correspond to the $\boldsymbol{3^{Fur}}$ and $\boldsymbol{3^{Pp}}$ PMMA thin films.

Experimental set-up and nonlinear optical measurements

The nonlinear optical response of the O-doped PAHs has been investigated employing 4 ns, visible (532 nm) and infrared (1064 nm) laser pulses using the Z-scan technique. Z-scan was selected because it is a powerful and relatively simple experimental technique which allows for the simultaneous determination of the sign and the magnitude of the NLO absorption and refraction of a sample (*i.e.*, the NLO absorption coefficient, β, and the NLO refractive

parameter, γ') both derived from a single measurement. Since a detailed description of the Z-scan technique can be found elsewhere,[13,14] only a short description will be presented here. So, briefly, in this technique the transmittance of a sample is measured using two different experimental configurations, as it moves along the propagation direction (*e.g*. the z-axis) of a focused Gaussian laser beam experiencing different laser intensity at each z-position. The two configurations are named "open-aperture" (OA) and "closed-aperture" (CA) Z-scan. In the former, the transmittance is measured by collecting the transmitted laser beam just after the sample while in the latter, the transmittance is measured by collecting a part of the laser beam after it has passed through a finite aperture placed in the far field. From the OA and CA transmittance measurements, the NLO absorption coefficient β (m/W) and the NLO refractive parameter γ' (m^2/W) can be deduced. So, from the OA Z-scan, both the sign and the magnitude of β can be deduced after fitting the OA Z–scan with the following equation:

$$T(z) = \frac{1}{\sqrt{\pi}\dfrac{\beta I_0 L_{eff}}{\left(1+z^2/z_0^2\right)}} \int_{-\infty}^{+\infty} \ln\left[1+\frac{\beta I_0 L_{eff}}{\left(1+z^2/z_0^2\right)}\exp\left(-t^2\right)\right] dt \qquad (1)$$

where T is the normalized transmittance, I_0 is the on-axis peak intensity of the laser beam at the focus, z_0 is the Rayleigh length and L_{eff} is the effective thickness of the sample given by the formula: $L_{eff} = (1-e^{-a_0 L})/a_0$, with α_0 being the linear absorption coefficient at the laser wavelength and L denoting the thickness of the sample.

The absorption coefficient α_0 of a sample was calculated from the following relation: $\alpha_0\left(cm^{-1}\right) = ln10 \times \dfrac{A}{L(cm)}$, where A is the absorbance of the sample at the excitation wavelength, *i.e*., at 532 nm, measured with the spectrophotometer and L as defined above. For solutions contained in 1 mm pathlength cells, it holds that L=0.1 cm and α_0 was calculated to be between 0.02 and 11 cm^{-1}, corresponding to an L_{eff} of about 0.1 cm. However, for the thin films, having

a thickness (L) of few hundreds nm, the α_0 is calculated to be 43 to 14200 cm^{-1}, resulting to an L_{eff} of few hundreds nm depending on the PAH.

Positive (or negative) sign NLO absorption coefficient β (corresponding to reverse saturable absorption-RSA or saturable absorption-SA) are indicated by the presence of a minimum (or a maximum) in the OA Z-scan transmittance recording.

From the CA Z-scans, exhibiting a pre-focal minimum followed by a post-focal maximum (*i.e.*, valley-peak, $Re\chi^{(3)}>0$) or a pre-focal maximum followed by a post-focal minimum (*i.e.* peak-valley, $Re\chi^{(3)}<0$), the NLO refractive index parameter γ' can be deduced. In the former situation, the sample acts as a positive lens, focusing the transmitted laser beam, while in the latter case, the sample acts as negative lens, causing defocusing of the transmitted laser beam. Both focusing and defocusing phenomena take place around the focal plane, where the sample experiences the highest incident laser intensity.

For weak or negligible absorption, the nonlinear refractive index parameter γ' can be obtained from the CA Z-scan using the following equation:

$$\gamma' = \frac{\lambda \alpha_0}{1-e^{-\alpha_0 L}} \frac{\Delta T_{p-v}}{0.812\pi I_0 \left(1-S\right)^{0.25}} \qquad (2)$$

where λ is the laser wavelength, $\Delta T_{\text{p-v}}$ is the difference between the peak and the valley of the normalized transmittance, S is the linear transmittance of the aperture (defined as: S=1–exp(-$2r_a^2/w_a^2$); with r_a being the radius of the aperture and w_a being the beam radius at the aperture). The quantities α_0, I_0 and L are as defined previously.

If absorption is not negligible, then γ' is obtained from the *"divided"* Z-scan (denoted as "D" in the next), which results from the division of the OA by the corresponding CA Z-scan.

Then, with the nonlinear optical parameters β and γ' known, the imaginary ($Im\chi^{(3)}$) and real ($Re\chi^{(3)}$) parts of the third-order nonlinear susceptibility, $\chi^{(3)}$, can be calculated from the following relations:

$$\mathrm{Re}\,\chi^{(3)}(esu) = 10^{-6}\frac{c n_0^2}{480\pi^2}\gamma' \ (\mathrm{cm}^2/\mathrm{W}) \text{ and } \mathrm{Im}\,\chi^{(3)}(esu) = 10^{-7}\frac{c^2 n_0^2}{96\pi^2\omega}\beta \ (\mathrm{cm}/\mathrm{W}) \quad (3)$$

where ω (in s^{-1}) is the frequency of the laser light.

The magnitude of third-order nonlinear susceptibility, $\chi^{(3)}$, is easily calculated then, from the known $Im\chi^{(3)}$ and $Re\chi^{(3)}$. However, since $\chi^{(3)}$ depends on the number density N, often the second hyperpolarizability, γ (in esu), is used, which is defined as: $\gamma = \chi^{(3)}/NL^4$, where L is the Lorentz–Lorenz local field correction factor defined as: $L = \left(n_0^2 + 2\right)/3$ and n_0 the refractive index of the solvent, can be more useful, as it describes the nonlinearity per molecule, which is a molecular constant, independent of N, simplifying the direct comparison of the NLO response of different molecules.

All measurements presented here were performed using a Q-switched, 4 ns Nd:YAG laser as an excitation source. The laser had a gaussian spatial profile and was operating between 1 and 10 Hz. Measurements were performed using both its second harmonic output at 532 nm and its fundamental output at 1064 nm. The laser beam was focused into the samples by means of a quartz 20 cm plano-convex lens, while the beam waist at the focal plane was determined using a CCD camera and was found to be 18/30 μm at 532/1064 nm respectively.

Results and Discussion

For the determination of the nonlinear optical parameters β, γ', the third-order nonlinear susceptibility $\chi^{(3)}$ and the elucidation of the physical origins of the NLO response, Z-scan measurements of solutions of O-doped PAHs at different concentration were performed at several incident laser energies. In addition, in order to study the NLO response of O-doped PAHs in a different matrix environment, interesting for several applications, thin PMMA films doped with different amounts of each PAH were prepared and measured by Z-scan. To account for the inhomogeneities of the thickness of a film, several measurements were performed at

different positions on the surface of each film; then the average value was used for the calculation of the NLO parameters.

Since the solvent used for the preparation of the solutions, *i.e.* toluene, was found to exhibit negligible NLO response for the range of laser intensities employed in these experiments, the NLO response of the PAHs solutions can be attributed exclusively to the PAH content of each solution. A similar situation was found for the thin films, where neat PMMA coated glass substrates did not exhibit any NLO response, thus the NLO response of the thin films being attributed to the PAH content of the film. The detailed results concerning the thin films will be discussed at the end of the section.

From the UV-Vis-NIR absorption spectra of the PAHs' solutions shown in Figure 2, their transparency for infrared wavelengths (*i.e.,* at 1064 nm) is easily seen, while in the visible (*i.e.,* at about 532 nm), the presence of some absorption is obvious, its magnitude depending on the PAH. Therefore, excitation with 1064 nm laser light is an off-resonant excitation process, while visible excitation meets the conditions of full- or near-resonant excitation condition depending on the PAH. In the latter case, an enhancement of the NLO response is expected in principle. Actually, this is the case for excitation of molecules $\boldsymbol{3^{Fur}}$, $\boldsymbol{3^{Pp}}$ and $\boldsymbol{2^{Pp}}$ with 532 nm laser light as will be discussed in the text.

In Figure 3, some representative OA and divided Z-scans of all studied PAHs are presented providing a qualitative picture summarizing their NLO absorptive and refractive behaviors. In more detail, the "divided" Z-scans of $\boldsymbol{1^{Fur}}$, $\boldsymbol{2^{Fur}}$, $\boldsymbol{1^{Pp}}$, $\boldsymbol{2^{Pp}}$ and $\boldsymbol{3^{Pp}}$ exhibited a peak-valley configuration, indicative of self-defocusing behavior, corresponding to negative NLO refractive index parameter γ' (*i.e.* $\mathrm{Re}\chi^{(3)}<0$), while PAH $\boldsymbol{3^{Fur}}$ exhibited negligible nonlinear refraction, completely suppressed by its strong absorption at 532 nm, due to the proximity of the excitation with the origin of its π-π* absorption band located at 534 nm. On the opposite side, PAHs $\boldsymbol{1^{Fur}}$ and $\boldsymbol{1^{Pp}}$ exhibited very weak NLO refraction due to the off-resonant character

of their excitation. In this case, to improve the signal to noise ratio, much higher concentration solutions, compared to the solutions of the other PAHs, were prepared and used for the measurements (see e.g. Table S1). From the determined values of the nonlinear refractive index parameter γ', by taking into account the concentrations of the solutions used (see e.g. Table S1), by looking at the UV-Vis-NIR absorption spectra of the PAHs presented in Fig. 2 and the spectral position of the strongest band (see Table S1), it is evident that $\boldsymbol{2^{Pp}}$ or $\boldsymbol{3^{Pp}}$ exhibit significant enhancement of their NLO refractive response compared to that of $\boldsymbol{1^{Pp}}$, which can be attributed to the increasing resonant character of the excitation. In fact, $\boldsymbol{2^{Pp}}$ and $\boldsymbol{3^{Pp}}$ exhibit an increase of their γ' values of about 5×10^3 and 10^3 respectively compared to that of $\boldsymbol{1^{Pp}}$, while the latter exhibits an NLO refraction of about 10 time stronger than that of $\boldsymbol{1^{Fur}}$. These experimental evidences clearly demonstrate the effect of the resonant enhancement on the NLO response. It is interesting to notice that even in the case of $\boldsymbol{1^{Fur}}$and $\boldsymbol{1^{Pp}}$, where the 532 nm laser excitation was occurring very far from any resonance band (i.e. 357 nm, 444 nm) and despite the as low as possible incident intensities employed, all measurements confirmed the presence of a clear defocusing behavior. To further investigate the presence of any thermal effects due to the laser energy deposited in the solution (because of any possible absorption at 532 nm), which can cause local heating resulting in defocusing behaviour, Z-scan measurements of all studied PAHs using different repetition rates of the laser, from 0.5 to 10 Hz, were performed. However, even for $\boldsymbol{3^{Fur}}$ and $\boldsymbol{2^{Pp}}$, whose strong absorption band is close to the excitation wavelength, no observable changes either of the shape and/or the $\Delta T_{p\text{-}v}$ parameter of the Z-scan scans were observed, suggesting the absence of such origin thermal effects in all cases.

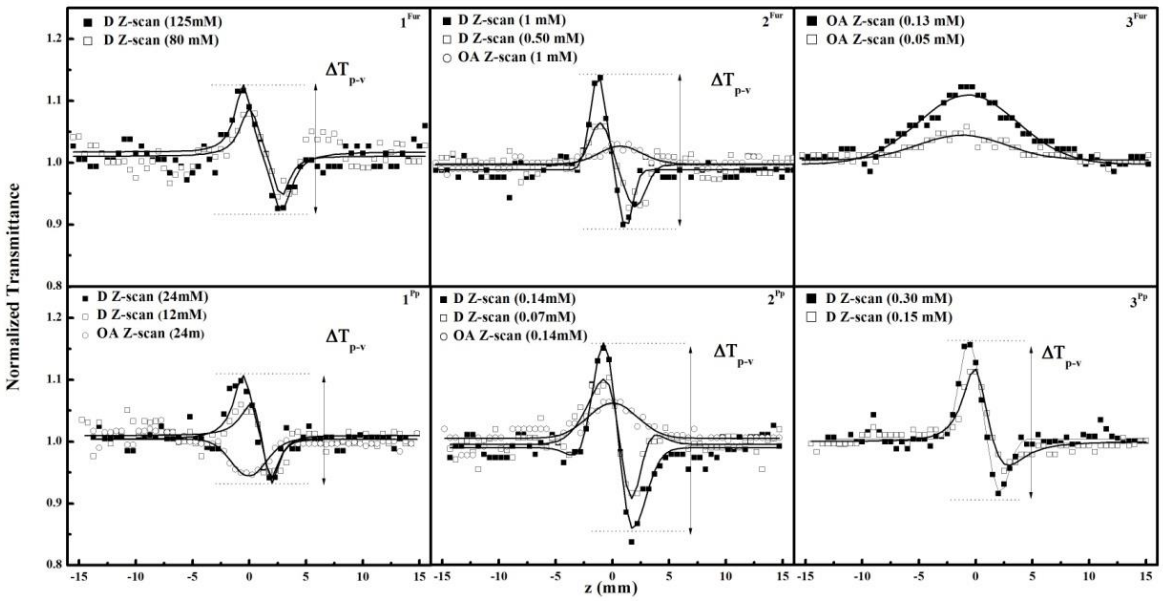

Figure 3. OA and D Z-scans of some toluene solutions of the furanyl and pyranyl PAHs: ***1***^{Fur}, ***2***^{Fur}, ***3***^{Fur}, ***1***^{Pp}, ***2***^{Pp} and ***3***^{Pp} under 532 nm, 4 ns laser excitation.

In Figure 4, the variation of the $\Delta T_{p\text{-}v}$ parameter is shown as it was deduced from 'divided' Z-scans of various concentration solutions performed using different incident laser intensities. As shown, all solutions' $\Delta T_{p\text{-}v}$'s were found to scale linearly with the laser intensity, suggesting third-order NLO response, while higher concentration solutions, resulted to steeper slopes implying larger NLO response, as expected. From the slopes of the continuous lines, corresponding to the linear best fit of the experimental data points, the nonlinear refractive index parameter γ' of each solution was determined using equation (2).

Concerning the nonlinear absorption, all PAHs were found exhibiting NLO absorption, its magnitude and sign dependent on the relative position of the origin of their π-π* absorption band from the excitation laser wavelength. This π-π* absorption band is a characteristic feature of all these PAHs and appears prominently in their UV-Vis-NIR absorption spectra as shown in the spectra presented in Figure 1. The exact locations of these band origins, are reported in the Table S1 of the Supporting Information (SI) (denoted as λ_{max}).

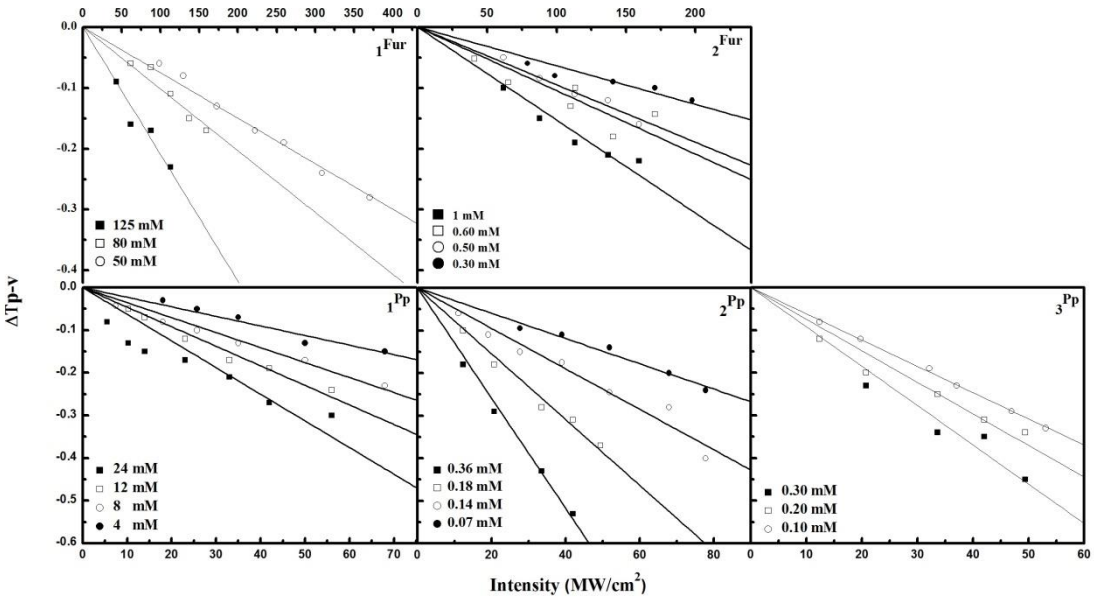

Figure 4. Variation of the $\Delta T_{p\text{-}v}$ parameter of the O-doped PAHs with the incident laser intensity under 532 nm, 4 ns laser excitation.

The present measurements demonstrate clearly the effect of the resonant excitation on the magnitude and the sign of the nonlinear absorption coefficient β. So, when the laser excitation wavelength was resonant or near-resonant with the origin of the π-π* band of the PAH, SA response was exhibited (*i.e.*, β<0). As shown in Figure 3, ***2*^{Fur}**, ***3*^{Fur}** and ***2*^{Pp}** exhibited SA behavior, while the ***1*^{Pp}** displayed a weak RSA response. The SA behavior of the former PAHs is attributed to the resonant excitation conditions, while ***1*^{Pp}**'s RSA behavior is understandable by invoking the participation of excited states with absorption cross section larger than that of the ground state, a situation similar to the RSA behavior of fullerene C_{60} (when excited with nanosecond visible laser pulses[13]) and some fully conjugated tri(perylene bisimides)[15] (often used as model systems for the investigation of the structure-property relationships of functionalized graphene nanoribbon (F-GNR) structures). It is only very recently, that this hypothesis about ***1*^{Pp}** (*peri*-xanthenoxanthene, PXX) has been confirmed

experimentally, by transient absorption measurements, attesting the presence of a relatively long-lived (>~3 μs) triplet state.[16]

Concerning the PAHs ***1^Fur*** and **3^Pp**, they both exhibited negligible nonlinear absorption, as expected, since the excitation was taking place far enough from their π-π* bands. Especially for ***1^Fur***, although solutions of much higher concentration have been prepared and measured, compared to the solutions of the other PAHs, its NLO absorption was too weak to be accurately determined; from the analysis of the measurements, an upper limit of the NLO absorption was estimated, ranging between 0.1 and 0.5 of the value of its homologue ***1^Pp***. Similarly, systematic attempts to measure the NLO response of all studied PAHs under infrared 1064 nm excitation, have confirmed their very low response under infrared excitation, although an order of magnitude larger incident laser intensities and concentrations were used compared to those employed under visible excitation.

In Figure 5, the variation of the NLO absorption coefficient β versus the incident laser intensity of some selected PAHs' solutions is depicted. For most of the PAHs studied, β was found to be practically constant with the laser intensity, as it should be in the case of a pure two-photon absorption (TPA) process assuming virtual states; in this case, β should be constant and independent on the laser intensity, depending only on the ground state population N_g, since the absorption coefficient corresponds to the product of the absorption cross section σ by N_g. Since, σ is a microscopic parameter, independent of N_g, a change in β will be evident only when there is a substantial change in N_g e.g. due to the absorption. Therefore, if the absorption is weak, then β can be considered as a constant, since there is a negligible change of the ground state population N_g. Considering that TPA is a very weak phenomenon usually, the corresponding NLO absorption coefficient β can be considered as a constant[17,18] which is characteristic of the material. However, if there is an important excited state absorption (ESA) during a TPA process, then significant depletion of the ground state population N_g can occur.

Then, the NLO absorption coefficient β can exhibit a variation with the laser intensity. Usually, under ns excitation, the NLO absorption coefficient β is found decreasing suggesting the presence of an ESA process.[18]

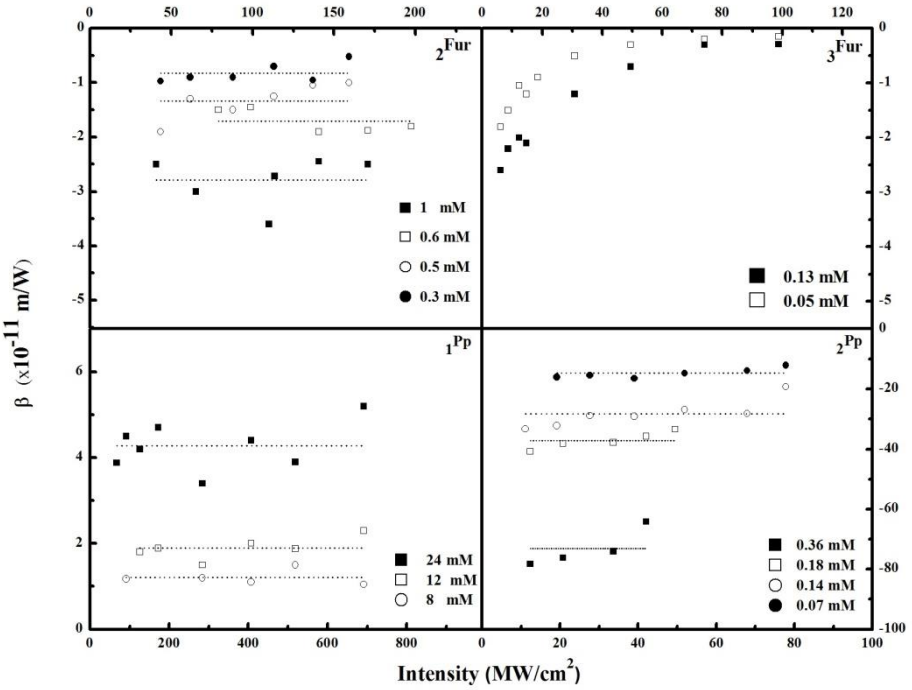

Figure 5. Variation of the nonlinear absorption coefficient β of the O-doped PAHs with the incident laser intensity under 532 nm 4 ns laser excitation.

Although the detailed photophysics of the investigated PAHs is incomplete to the best of our knowledge, for some of them a partial knowledge about their optical properties has been reported [11,16] permitting some initial conclusions to be drawn concerning the physical mechanisms responsible for the NLO response. So, based on the experimental evidences, a two-photon absorption mechanism (TPA) can be reasonably assumed. In general, following a two-photon excitation, the molecule can fluoresce from the singlet excite state with a certain quantum yield Φ or relax back to the ground state *via* nonradiative processes (within time scales of ~(10^{-11}–10^{-8}) s) or it can be further excited within the manifold of the singlet excited states

or after undergone intersystem crossing to be transferred to a triplet state and then follow further excitation within the manifold of triplet states. In addition to the cross sections of these processes, the pulse duration and shape and the intensity of the incident radiation will also determine the details of the NLO response. So, if the fluorescence lifetime, *t*, is comparable with or longer than the laser pulse duration, t_{laser}, *i.e.* $t \geq t_{laser}$, or if the photon flux is very high, the population of the excited state can be large enough during the pulse so that other processes can occur and grown up, becoming competitive with the radiative and non-radiative relaxation pathways.[19] For instance, for a long living singlet excited state population, further excitation is possible through the singlet or the triplet states (e.g. after efficient and fast intersystem crossing, etc.). In the case of the present PAHs, the radiative deactivation times of their singlet excited states (see e.g. Table 1) fall in the 2–6 ns range, and are comparable to the duration of the excitation laser pulse. Therefore, under the present experimental conditions and for the laser intensities employed, it can be assumed that enough population remains in the singlet state during the excitation, making the absorption of one more photon possible, resulting to the depletion of this state finally and resulting to saturable absorption. Simultaneously, depletion of the ground state of the PAH, although it cannot be completely ruled out, it seems less probable due to the relatively low laser intensities employed. The proposed scheme can explain both the SA behavior and the constant NLO absorption coefficient β implying a TPA process. Furthermore, the nonlinear absorption coefficient β was found to depend linearly on the concentration of the solution for the range of concentrations and the incident laser intensities employed as should be expected.[19,20]

An exception from the above trend was observed for $\boldsymbol{3^{Fur}}$, where β was found to vary with the laser intensity, attaining a constant value for high incident laser intensities. However, this behaviour can be understood in terms of the resonant excitation occurring in the case of

***3**^{Fur}* resulting to the depletion of the ground state. In this case, an intensity-dependent absorption coefficient *α(I)* is usually considered having the following form:[20–22]

$$\alpha(\mathrm{I}) = \frac{\alpha_0}{1 + \mathrm{I}/\mathrm{I}_s} \qquad (4)$$

where α_0 (cm^{-1}) is the linear absorption coefficient and I_s is the saturation intensity (*i.e.* the intensity for which the absorption coefficient *α(I)* reduces to half of its value at the low-intensity regime).

Since the intensity dependent absorption *α(I)* of a material exhibiting third-order NLO response is related to the nonlinear absorption coefficient *β* through the relation: $\alpha(\mathrm{I}) = \alpha_0 + \beta I$, an intensity-dependent nonlinear absorption coefficient *β* results described by a relation of the following form:

$$a(I) = \frac{a_0}{1 + (I / I_s)} + \beta I \qquad (5)$$

So, in the case of the toluene solutions of ***3**^{Fur}*, the corresponding nonlinear absorption coefficient *β* was determined from this last relation. The saturation intensity I_s was determined and found to be $46.8 \pm 0.5 \times 10^9$ W/m^2.

The variation of the third-order susceptibility $\chi^{(3)}$ with the concentration of the O-doped PAH is presented in Figure 6. As shown, the third-order susceptibility was found to increase linearly with the concentration of the PAH, confirming the consistency of the measurements and the absence of any unwanted effects (e.g., saturation effects, aggregation, etc.). The real and imaginary parts and the magnitude of the third-order susceptibility $\chi^{(3)}$ of studied PAHs' solutions are presented in detail in Table S1 of the SI. From the slopes of the straight lines, corresponding to the linear best fit of the experimental data points, the second hyperpolarizability value, *γ*, is deduced for each O-doped PAH, a quantity which is do not depend on the concentration and is considered as a molecular property revealing the strength of the NLO response of a molecule. The deduced second hyperpolarizability values of the

investigated PAHs are presented in Table 1. As can be seen, ***3***^{Fur}, ***3***^{Pp} and ***2***^{Fur}, ***2***^{Pp} exhibited the largest second hyperpolarizabilities, followed by ***1***^{Fur} and ***1***^{Pp}. The very large values of ***3***^{Fur}, ***3***^{Pp} *and* ***2***^{Pp} are due to the resonant or near-resonant situation occurring under visible (532 nm) laser excitation. In fact, increasing the number of naphtalene units on the molecular scaffold, *e.g*. going from molecule ***1*** to ***3***, two important consequences are occurring on these PAHs. At first, their electronic excited states are shifted to lower energy, making the excitation with visible photons to acquire more resonant degree; simultaneously, an increasing of the charge delocalization over the molecular scaffold takes place, resulting in enhancing the NLO response as well. The combined action of these two factors results in an enhancement of the second hyperpolarizability of ***3***^{Fur} of about 28×10^3 times compared to ***1***^{Fur}, the latter PAH presenting the weaker second hyperpolarizability among the investigated ones.

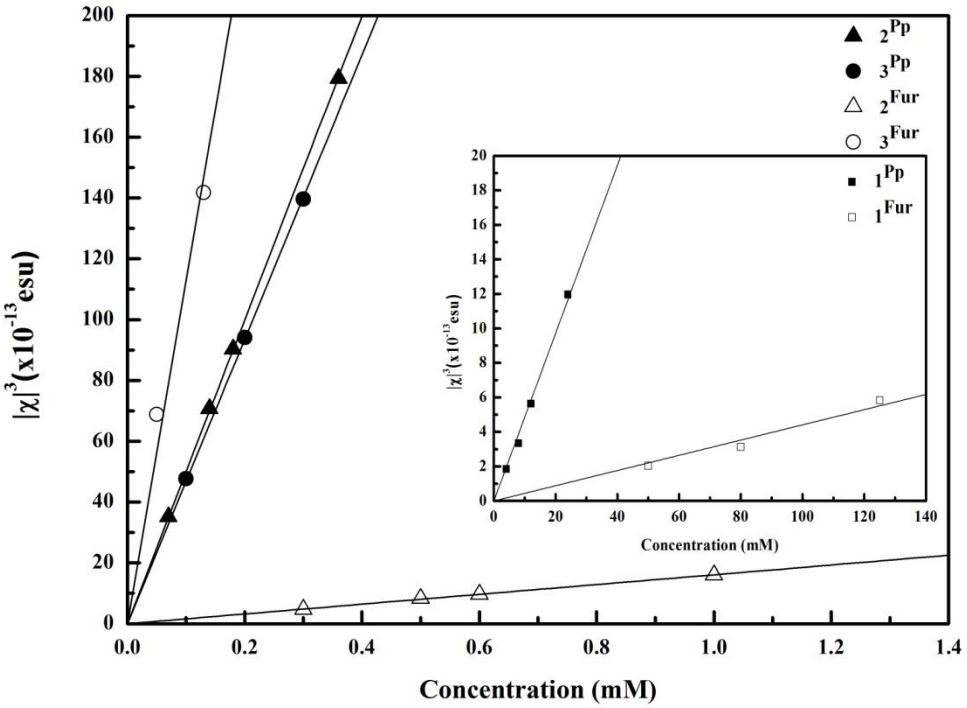

Figure 6. Dependence of the third-order nonlinear susceptibility, $\chi^{(3)}$, on the concentration of the O-doped PAHs under 532 nm 4 ns laser excitation.

Another parameter that greatly affects the NLO response of investigated PAHs, is the degree of planarity.[11,16,23] On its turn, the degree of planarity of a molecular scaffold can affect importantly the transition dipole moment of a transition, making a transition to acquire more/less forbidden character, increasing/decreasing respectively its radiative lifetime, thus having a direct influence on the NLO response. The present results provide an undoubtful experimental evidence that higher planarity PAHs possess larger second hyperpolarizability value demonstrating one more strategy for the efficient tuning of the NLO response of a molecular system. In that view, comparing for example the γ values within the furanyl/pyranopyranyl homologues ***1***^{Fur}/***1***^{Pp} and ***2***^{Fur}/***2***^{Pp} it becomes evident that the pyranopyranyl systems exhibit systematically larger second hyperpolarizability than their furanyl homologues. This conclusion seems to be unsatisfied examining *e.g*. the couple of PAHs ***3***^{Fur} *and* ***3***^{Pp}; however, in this case, the incidence of full resonant excitation condition holding for ***3***^{Fur}, whose π-π* band is at 534 nm, conceals the effect of planarity on the NLO response. Along these lines, it would be interesting to examine the effect of the replacement of O-atom(s) by heavier atom(s), as for instance sulfur (S) or selenium (Se), which might affect the planarity of these PAH, thus improving the second hyperpolarizability values.

Table 2. Second hyperpolarizability (γ) values of the O-doped PAHs

PAH (λ_{max})[a]	**Reγ** (×10^{-31} esu)	**Imγ** (×10^{-31} esu)	**γ** (×10^{-31} esu)	**γ** (×10^{-31} esu)	**Imγ** (×10^{-31} esu)	**Reγ** (×10^{-31} esu)	**PAH** (λ_{max})[a]
1^{Fur} (357)	-	-	0.0165±0.00	0.193±0.02	0.040±0.00	-	***1***^{Pp} (444)
2^{Fur} (477)	-6.58±0.4	-1.29±0.1	6.69±0.4	208.7±20.0	-48.78±6	-	***2***^{Pp} (556)
3^{Fur} (534)	-	-512.9±40	512.9±40	195.8±30.0	-	-	***3***^{Pp} (639)

[a] Wavelength of the lowest-energy electronic transition in toluene.

Thin film results

For the completeness of the present study towards the potential use of the present O-doped PAHs in applications, the assessment of their NLO response when embedded in a solid matrix was also performed. For this, Z-scan measurements of PMMA thin films, doped with different amounts of PAHs and having different thicknesses were prepared. Representative UV-Vis-NIR absorption spectra of the prepared films are presented in the SI. In order to avoid local heating or destruction of the films during the measurements, the laser repetition rate was set of 1 Hz. In Figure 7, an example of the OA and "divided" Z-scans of a 390 nm thick PMMA film doped with ***2***^{Pp} under 532 nm laser excitation is presented. As shown, the ***2***^{Pp} films exhibited RSA behavior, (*i.e.* $\beta>0$) and defocusing (*i.e.* peak-valley configuration, $\gamma'<0$). Similar behaviour was found for ***3***^{Pp} and ***3***^{Fur}, the latter however exhibiting saturable absorption ($\beta<0$), due to the close proximity of the 532 nm excitation with the origin of its π-π* band, the excitation being practically in resonance. Thin films of ***1***^{Fur}, ***1***^{Pp} and ***2***^{Fur} were found to lack of sizable or systematic NLO response, at least for the range of laser energies employed (*i.e.* up to 22 μJ, corresponding to laser intensity of ~260 MW/cm^2). The absence of significant NLO response of ***1***^{Fur} and ***1***^{Pp} films can be attributed to their intrinsic weak NLO response, which is in full agreement with the results obtained for their toluene solutions. Additionally, the locations of their π-π* bands, *i.e.* at 357 and 444 nm respectively, makes their excitation with 532 nm laser radiation substantially less efficient, being a typical non-resonant process. Similar behavior was found for the films of ***2***^{Fur} which exhibited very weak NLO response as their π-π* band is located at 477 nm, considerably far from the excitation wavelength. This situation could be overcome using thicker films, however, in this case, the homogeneity and optical quality of the films were unsuccessful.

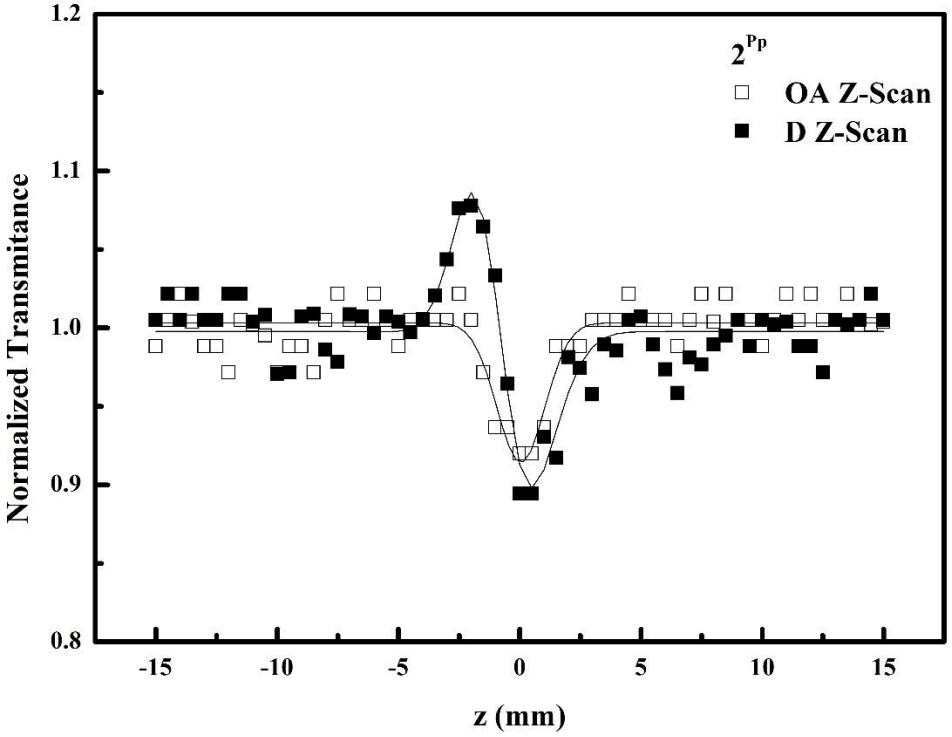

Figure 7. OA and D Z-scans of a 390 nm thick PMMA film (1000 rpm, 30 s, 3.2 mM) doped with ***2^{Pp}*** under 532 nm, 4 ns laser excitation.

In Figure 8, the dependence of the $\Delta T_{p\text{-}v}$ parameter on the incident laser intensity is presented for some PMMA films doped with ***2^{Pp}***, ***3^{Pp}*** and ***3^{Fur}*** under 532 nm laser excitation. As shown, all films exhibited sizeable defocusing behavior, with the furanyl one exhibiting the stronger response, while the pyranopyranyl PAHs films exhibited relatively weaker response. It is interesting to notice that the solutions of ***3^{Fur}*** exhibited negligible NLO refraction due to the strong resonant absorption they exhibit (as their π-π* band lies at 534 nm, that is only 2 nm away from the laser excitation wavelength). However, in the case of films, as they are much thinner, the much weaker absorption they exhibit is only reducing their NLO refraction, without being capable to completely extinguish it.

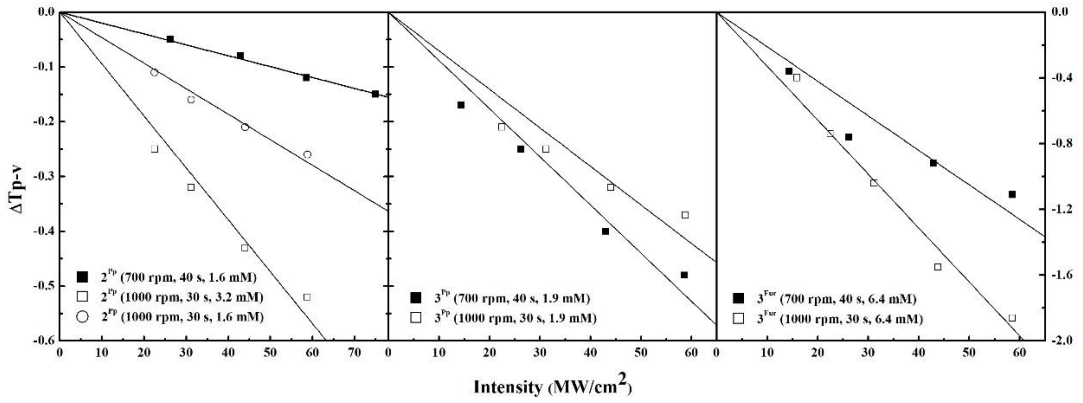

Figure 8. Variation of the $\Delta T_{p\text{-}v}$ parameter with the incident laser intensity for ***2^Pp***, ***3^Pp*** and ***3^Fur*** doped PMMA films under 532 nm, 4 ns laser excitation.

The dependence of the NLO absorption coefficient β on the incident laser intensity for the ***2^Pp***, ***3^Pp*** and ***3^Fur*** doped PMMA films is presented in Figure 9. As shown, ***2^Pp*** and ***3^Pp*** doped films exhibited RSA behavior, i.e. β>0, while the ***3^Fur*** films exhibited strong SA behavior, *i.e.* β<0, due to the resonant nature of the excitation, as the laser wavelength is resonant with the π-π* band (at 534 nm). The details of the measured NLO quantities and the experimental parameters used for the preparation of the thin films together with their thickness are summarized in Table S2 of the Supporting Information (SI).

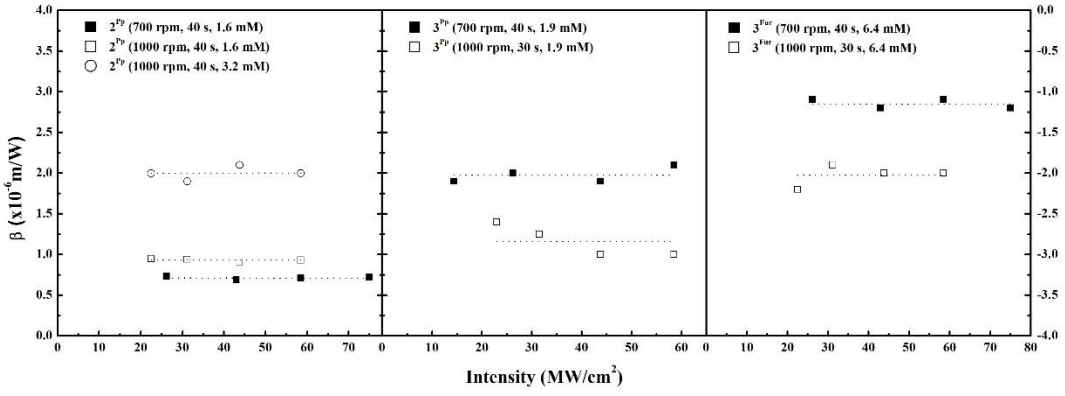

Figure 9. Variation of the nonlinear absorption coefficient β with the incident laser intensity for ***2^Pp***, ***3^Pp*** and ***3^Fur*** doped PMMA films under 532 nm, 4 ns laser excitation.

From the comparison of the results concerning the NLO properties of the PAHs obtained from the PMMA films with those from toluene solutions, it is obvious that the studied PAHs maintain their NLO properties in both environments without any degradation of their NLO response. This finding is of high importance and is very promising fact for the use of the present PAHs in photonic applications.

Conclusions

In the present work, the nonlinear optical response of O-doped PAHs ***1-3***$^{Fur/Pp}$ has been systematically investigated and their third-order nonlinear optical properties were determined under 4 ns, visible (532 nm) excitation. They were found displaying important NLO negative sign absorption and refraction, both increasing with the addition of naphtalene units and with the number of O-atoms. In particular, among the furanyl derivatives, an enhancement of the second hyperpolarizability of more than 30×10^3 times was found for ***3***^{Fur} compared to ***1***^{Fur}. Correspondingly, for the pyranopyranyl derivatives, an enhancement of the second hyperpolarizability of about 10^3 times was observed between ***1***^{Pp} and ***3***^{Pp}. Most of the studied PAHs exhibited saturable absorption behavior due to the resonant excitation conditions. The investigated PAHs were found to exhibit negligible NLO response under infrared (1064 nm) excitation.

Supporting Information

Absorption spectra of the investigated samples in thin film form and tables with the analytical data from the experiments

Acknowledgements

JP acknowledges "*Advancing Young Researchers' Human Capital in Cutting Edge Technologies in the Preservation of Cultural Heritage and the Tackling of Societal Challenges*

– *ARCHERS*" project of Stavros Niarchos Foundation for partial support. ZB acknowledges partial support from the "*Investigation of the Non-Linear Optical Response of Graphene's Derivatives with the Z-scan Technique*" (MIS 5002556) which is implemented under the "*Action for the Strategic Development on the Research and Technological Sector*", funded by the Operational Programme "*Competitiveness, Entrepreneurship and Innovation*" (*NSRF 2014-2020*) and co-financed by Greece and the European Union (European Regional Development Fund). DB gratefully acknowledges Cardiff University.

References

1. Anthony, J. E. Functionalized acenes and heteroacenes for organic electronics. *Chem. Rev.* **2006**, *106*, 5028–5048.
2. Wu, J.; Pisula W.; Müllen K. Graphenes as potential material for electronics. *Chem. Rev.* **2007**, *107*, 718–747.
3. Zhan, X.; Facchetti, A.; Barlow, S.; Marks T. J.; Ratner M. A.; Wasielewski M. R.; Marder S. R. Rylene and related diimides for organic electronics. *Adv. Mater.* **2011**, *23*, 268–284.
4. Li, X.; Wang, X.; Zhang, L.; Lee, S.; Dai, H. Chemically derived, ultrasmooth graphene nanoribbon semiconductors. *Science.* **2008**, *319*, 1229–1232.
5. Petrushenko, I. K. DFT study on adiabatic and vertical ionization potentials of graphene sheets. *Adv. Mater. Sci. Eng.* **2015**, *2015*, 1–7.
6. Chen, L.; Hernandez, Y.; Feng, X.; Müllen, K. From nanographene and graphene nanoribbons to graphene sheets: Chemical synthesis. *Angew. Chemie - Int. Ed.* **2012**, *51*, 7640–7654.
7. Narita, A.; Feng, X.; Müllen, K. Bottom-up synthesis of chemically precise graphene nanoribbons. *Chem. Rec.* **2015**, *15*, 295–309.
8. Wang, X.; Sun, G.; Routh, P.; Kim, D. H.; Huangb, W.; Chen, R. Heteroatom-doped graphene materials: syntheses, properties and applications. *Chem. Soc. Rev.* **2014**, *43*, 7067–7098.
9. Nakanishi, K.; Sasamori, T.; Kuramochi, K.; Tokitoh, N.; Kawabata, T.; Tsubaki, K. Synthesis and properties of butterfly-shaped expanded naphthofuran derivatives. *J. Org. Chem.* **2014**, *79*, 2625–2631.
10. Nakanishi, K.; Fukatsu, D.; Takaishi, K.; Tsuji, T.; Uenaka, K.; Kuramochi, K.; Kawabata, T.; Tsubaki, K. Oligonaphthofurans: Fan-shaped and three-dimensional π-

compounds. *J. Am. Chem. Soc.* **2014**, *136*, 7101–7109.

11. Miletić, T.; Fermi, A.; Orfanos, I.; Avramopoulos, A.; Leo, F. D.; Demitri, N.; Bergamini, G.; Ceroni, P.; Papadopoulos, M. G.; Couris, S.; et al. Tailoring colors by O-annulation of polycyclic aromatic hydrocarbons. *Chem. - A Eur. J.* **2017**, *23*, 2363 – 2378.
12. Sciutto, A.; Fermi, A.; Folli, A.; Battisti, T.; Beames, J. M.; Murphy, D. M.; Bonifazi, D. Customizing photoredox properties of PXX-based dyes through energy level rigid shifts of frontier molecular orbitals. *Chem. - A Eur. J.* **2017**, *24*, 4382-4389.
13. Couris, S.; Koudoumas, E.; Ruth, A. A.; Leach, S. Concentration and wavelength dependence of the effective third-order susceptibility and optical limiting of C_{60} in toluene solution. *J. Phys. B At. Mol. Opt. Phys.* **1995**, *28*, 4537–4554.
14. Sheik-Bahae, M.; Said, A. A.; Wei, T.-H.; Hagan, D. J.; Van Stryland, E. W. Sensitive measurement of optical nonlinearities using a single beam. *Quantum Electron. IEEE J.* **1990**, *26*, 760–769.
15. Wang, H.; Su, H.; Qian, H.; Wang, Z.; Wang, X.; Xia, A. Structure-dependent all-optical switching in graphene-nanoribbon-like molecules: Fully conjugated tri(perylene bisimides). *J. Phys. Chem. A.* **2010**, *114*, 9130–9135.
16. Al-Aqar, R.; Benniston, A. C.; Harriman, A.; Perks, T. Structural dynamics and barrier crossing observed for a fluorescent O-doped polycyclic aromatic hydrocarbon. *ChemPhotoChem.* **2017**, *1*, 198–205.
17. Liaros, N.; Fourkas, J. T; The characterization of absorptive nonlinearities. *Laser Photonics Rev.* **2017**, *11*, 1700106-1700126.
18. Podila, R.; Anand, B.; West, J. P.; Philip, R.; Sai, S. S.; He, J.; Skove, M.; Hwu, S. J.; Tewari, S.; Rao, A. M. Evidence for surface states in pristine and Co-doped ZnO nanostructures: Magnetization and nonlinear optical studies. *Nanotechnology*. **2011**, *22*,

095703–095707.

19. Rumi, M.; Perry, J. W. Two-photon absorption: an overview of measurements and principles. *Adv. Opt. Photon*. **2010**, *2*, 451-518.

20. Anand, B.; Kaniyoor, A.; Swain, D.; Baby, T. T.; Rao, S. V.; Sai, S. S. S.; Ramaprabhu, S., Philip, R. Enhanced optical limiting and carrier dynamics in metal oxide-hydrogen exfoliated graphene hybrids. *J. Mater. Chem. C.* **2014**, *2*, 10116–10123.

21. Boyd, R. W. Nonlinear Optics. *Academic Press.* **2008**, 3rd edition, pp. 15.

22. Anusha, P. T.; Swain, D.; Hamad, S.; Giribabu, L.; Prashant, T. S.; Tewari, S. P.; Rao, S. V. Ultrafast excited-state dynamics and dispersion studies of third-order optical nonlinearities in novel Corroles. *J. Phys. Chem. C.* **2012**, *116*, 17828–17837.

23. Stassen, D.; Demitri, N.; Bonifazi, D. Extended O-doped polycyclic aromatic hydrocarbons. *Angew. Chemie - Int. Ed.* **2016**, *55*, 5947–5951.

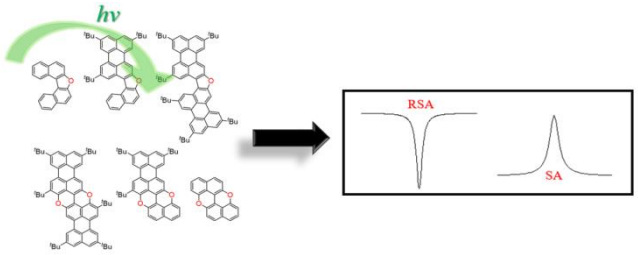

TOC Graphic